



Effect of aniline on cadmium adsorption by sulfanilic acid-grafted magnetic graphene oxide sheets



Xin-jiang Hu, Yun-guo Liu*, Guang-ming Zeng, Hui Wang, Xi Hu, An-wei Chen, Ya-qin Wang, Yi-ming Guo, Ting-ting Li, Lu Zhou, Shao-heng Liu, Xiao-xia Zeng

College of Environmental Science and Engineering, Hunan University, Changsha 410082, PR China

Key Laboratory of Environmental Biology and Pollution Control (Hunan University), Ministry of Education, Changsha 410082, PR China

ARTICLE INFO

Article history:

Received 18 January 2014

Accepted 5 April 2014

Available online 16 April 2014

Keywords:

GO-based composite

Sulfo group

Cadmium

Aniline

Mutual effect

ABSTRACT

Cd(II) has posed severe health risks worldwide. To remove this contaminant from aqueous solution, the sulfanilic acid-grafted magnetic graphene oxide sheets (MGOs/SA) were prepared and characterized. The mutual effects of Cd(II) and aniline adsorption on MGOs/SA were studied. The effects of operating parameters such as pH, ionic strength, contact time and temperature on the Cd(II) enrichment, as well as the adsorption kinetics and isotherm were also investigated. The results demonstrated that MGOs/SA could effectively remove Cd(II) and aniline from the aqueous solution and the two adsorption processes were strongly dependent on solution pH. The Cd(II) adsorption was reduced by the presence of aniline at pH < 5.4 but was improved at pH > 5.4. The presence of Cd(II) diminished the adsorption capacity for aniline at pH < 7.8 but enhanced the aniline adsorption at pH > 7.8. The decontamination of Cd(II) by MGOs/SA was influenced by ionic strength. Besides, the adsorption process could be well described by pseudo-second-order kinetic model. The intraparticle diffusion study revealed that the intraparticle diffusion was not the only rate-limiting step for the adsorption process. Moreover, the experimental data of isotherm followed the Freundlich isotherm model.

© 2014 Elsevier Inc. All rights reserved.

1. Introduction

Water pollution due to the indiscriminate disposal of different contaminants is a global environmental problem. For example, many industrial processes such as chemical manufacturing, battery manufacturing, metalliferous mining and leather tanning generate large quantities of wastewater containing various concentrations of Cd(II) [1]. Exceeding the micronutrient level of human body, Cd(II) ions affect the enzyme activity because of replacing Zn(II) ions in metallo-enzymes, and cause a number of acute and chronic disorders, such as renal damage, emphysema, hypertension, testicular atrophy and skeletal malformation in fetus [2,3]. For environmental protection, it is necessary to remove Cd(II) contaminated wastewater prior to its discharge to the environment. Compared with other disposal processes, adsorption is proved to be an effective method for the removal of toxic metal ions from wastewater as it is simple and economically viable.

A lot of organic and inorganic materials have been applied to remove various contaminants such as heavy metal ions and

organic substances. Attention has been focused on graphene oxide (GO) in recent years because it has a lot of oxygen-containing groups, such as hydroxyl, epoxide, carbonyl and carboxyl groups, which are essential for the high adsorption of contaminants. However, after the adsorption is carried out, the GO is difficult to be separated from the solution using traditional separation methods due to its hydrophilic nature [4]. The problem can be solved using magnetic technology. Actually, some studies had reported the synthesis of magnetic graphene oxide composites [5–8]. These composites were synthesized by loading magnetic nanoparticles on the GO sheets surface, which could be easily collected from water with the help of an external magnetic field. However, the loaded Fe₃O₄ particles on the GO surface may result in the loss of adsorption capacity because some groups of the GO are occupied by the magnetic nanoparticles. Several chemical reagents, such as EDTA [9] and ethylenediamine [10], demonstrated some positive benefits for enhancing the adsorption capacity of GO when they were used to modify the GO. Sulfanilic acid contains a sulfo group and an amino group, which can form stable chelates with metal ions. So, graft of sulfanilic acid on the magnetic graphene oxide surface may increase the adsorption ability of the composite.

It is well known that organic substances and metal ions are co-existing contaminants in wastewater, and organic substances can

* Corresponding author at: College of Environmental Science and Engineering, Hunan University, Changsha 410082, PR China. Fax: +86 731 88822829.

E-mail address: hnuese@126.com (Y.-g. Liu).

react with metal ions, thereby influencing the removal of metal ions [11]. Aniline is an important chemical compound which is well known for its wide applications in the manufacture of dyestuffs, rubbers, pesticides, plastics and paints [12]. It is frequently found in industrial effluents and surface water due to its disposal, which cause a series of environmental problems [13]. Aniline and Cd(II) are often used together in many industrial processes such as chemical manufacturing, leather tanning, dyeing, and rubber manufacturing. Therefore, there is a high possibility that aniline and Cd(II) ions exist in mixed contaminant systems. The amino group of aniline can form stable complexes with metal ions. Besides, the aniline can interact with GO-based composites through strong π - π interaction in aquatic systems [11]. Both of these may affect the adsorption behaviors of Cd(II) ions on GO-based composites.

The objectives of this study were to: (1) prepare and characterize sulfanilic acid-grafted magnetic graphene oxide sheets (denoted as MGOs/SA) and apply them as adsorbent for effective decontamination of Cd(II) from aqueous solution; (2) study the mutual effects of Cd(II) and aniline adsorption on MGOs/SA; (3) investigate the effects of the process parameters on Cd(II) adsorption; (4) study the adsorption mechanism with kinetics and isotherm models.

2. Materials and methods

2.1. Synthesis of MGOs/SA

Graphene oxide sheets (GOs) were prepared from natural graphite by modified Hummers method [14]. Briefly, 6 g graphite powder, 5 g $K_2S_2O_8$ and 5 g P_2O_5 were added into 24 mL of H_2SO_4 (98%) and stirred at 80 °C for 4.5 h. Then, 1 L of Milli-Q water was added and left overnight. The mixture was washed thoroughly and dried under vacuum at 60 °C. The residue was collected and put into 240 mL cold (0 °C) H_2SO_4 (98%), and then 5 g $NaNO_3$ and 30 g $KMnO_4$ were added gradually and the mixture was continually stirred below 20 °C for 4 h. Then, the reaction was carried out at

35 °C for 2 h. Next, 0.5 L of water was added slowly and the mixture was stirred for another 6 h at 90 °C. After that, 1 L water and 40 mL H_2O_2 (30 wt.%) were added to the mixture, and stirred for 2 h at room temperature. The paste was washed repeatedly with HCl (10%) and Milli-Q water and then sonicated for 2 h and a GOs solution was obtained. The magnetic graphene oxide sheets (MGOs) were prepared by coprecipitating Fe^{2+} and Fe^{3+} ions with ammonia solution in the GOs solution [8]. Typically, 200 mL mixed solution of $FeCl_3$ (0.1 mol/L) and $FeCl_2$ (0.05 mol/L) was added to 400 mL GOs solution (5 mg/mL) with stirring. Chemical precipitation was achieved at 85 °C under vigorous stirring by addition of ammonia solution and the pH was kept to 10 for 45 min. Then the sample was rinsed with Milli-Q water until the solution was neutral and a MGOs suspension was obtained. The sulfanilic acid-grafted magnetic graphene oxide sheets were synthesized from MGOs suspension in aryl diazonium salt solution [15]. The diazonium salt solution was prepared as the following: 0.5 g of sulfanilic acid and 0.4 g of $NaNO_2$ were added to 20 mL NaOH solution (1%), and then 20 mL ice water and 1 mL of concentrated HCl were added into the mixed solution and stirred for 20 min at 0 °C. Next, the diazonium salt solution was added to 400 mL MGOs suspension in an ice bath and stirred for 4 h. The obtained MGOs/SA were rinsed with Milli-Q water for several times and stored at room temperature. Fig. 1 shows the preparation sketch of MGOs/SA.

2.2. Characterization

The X-ray diffraction (XRD) pattern of the MGO/SA composites was obtained on a Rigaku D/max-2500 diffractometer equipped with a rotating anode and Cu $K\alpha$ source. The magnetic property was characterized by magnetization curve using a vibrating sample magnetometer (Lake Shore 7410, USA). The morphology of the MGOs/SA was characterized by field-emission scanning electron microscopy (FESEM, JSM 6700F, Japan). The zeta potential of MGOs/SA was obtained by Zeta Sizer and Nano series equipped with a microprocessor unit (ZEN3690, Malvern, UK).

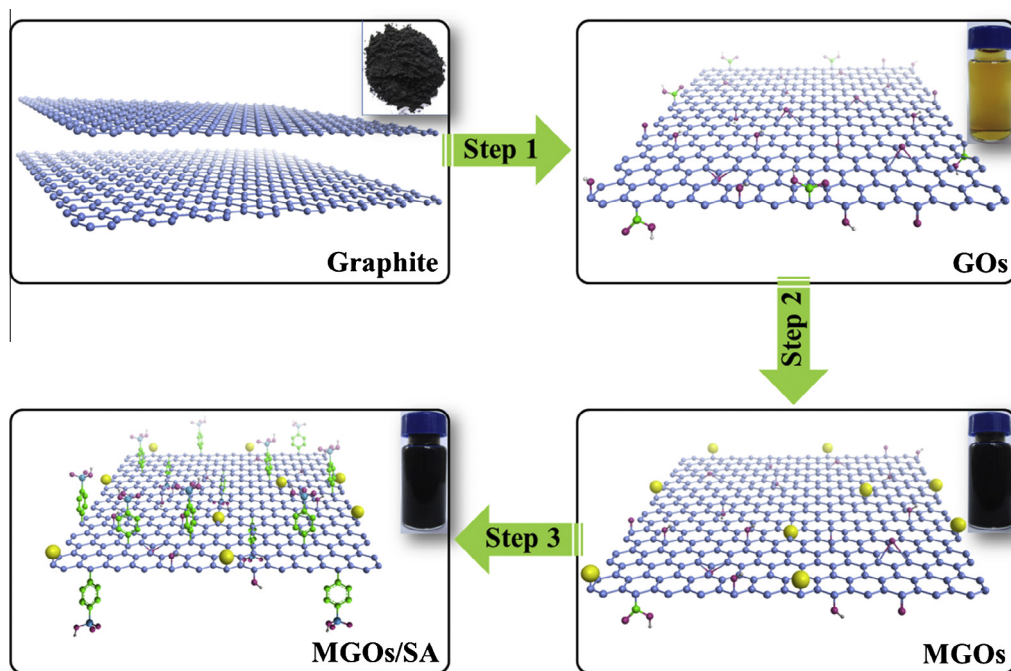


Fig. 1. Schematic representation of the synthesis processes of MGOs/SA from graphite: (Step1) oxidation of natural graphite to graphite oxide, followed by ultrasonication; (Step2) preparation of MGOs by loading magnetic nanoparticles on the GOs surfaces through chemical coprecipitation method; (Step3) formation of MGOs/SA by grafting sulfanilic acid on the MGOs surfaces.

2.3. Batch adsorption procedures

All adsorption experiments were performed according to the batch method in conical flasks on an orbital shaker with a shaking speed of 180 rpm. The stock solutions of Cd(II) and the stock suspension of the MGOs/SA were added to achieve the desired concentrations of the different components. After mixed for 24 h, the mixture was separated by a magnetic process using a permanent magnet. The Cd(II) concentration in the supernatant was analyzed using flame atomic absorption spectrometry (PerkinElmer AA700, USA). The concentration of aniline was determined by a UV–vis spectrophotometer (Shimadzu, UV-2550, Japan) at 280 nm [16]. The adsorption capacity (q_e) [$q_e = (C_0 - C_e) \times V/m$] (here, V is the volume of the suspension and m is the mass of MGOs/SA), adsorption percentage (E_e) [$E_e = (C_0 - C_e) \times 100/C_0$] and distribution coefficient (K_d) [$K_d = q_e/C_e$] of Cd(II) or aniline adsorbed on MGOs/SA were calculated from the difference between the initial concentration (C_0) and the equilibrium concentration (C_e) [17,18].

3. Results and discussion

3.1. Characterization of MGOs/SA

Fig. 2A shows the XRD spectrum of MGOs/SA. From the spectrum, seven major peaks at $2\theta = 30.10, 35.42, 37.05, 43.05, 53.39, 56.94$ and 62.52 are observed and can be assigned to diffraction from the (220), (311), (222), (400), (422), (511) and (440) planes of the cubic spinel crystal structure of Fe_3O_4 (JCPDS Card No. 19-0629) [19]. To study the magnetic properties of the MGO/

SA composites, the room-temperature magnetization hysteresis curve was measured using vibrating sample magnetometry (VSM). As shown in Fig. 2B, the magnetic hysteresis loop is S-like curve. The saturation magnetization (M_s), coercivity (H_c) and retentivity (M_r) are 15.24 emu/g, 5.15 Oe and 0.10 emu/g, respectively. Extremely small retentivity (nearly zero) of the sample indicated that there was almost no remaining magnetization when the external magnetic field was removed, suggesting that MGOs/SA exhibit superparamagnetic behavior at room temperature [20]. The insets in Fig. 2B show that the obtained MGOs/SA can be collected by a permanent magnet from aqueous solution. This property is important for the convenient recycling of these MGOs/SA. Cd(II) is first adsorbed onto the MGOs/SA to achieve equilibrium, and then the pollutants-loaded MGOs/SA are attracted by a magnet and the clear solution can be decanted off or removed by pipet. The result confirms that the MGOs/SA are magnetic and can potentially be used as an magnetic adsorbent to remove pollutants in liquid-phase processes. The FESEM image of MGOs/SA is demonstrated in Fig. S2 (Supplementary data). The image shows that Fe_3O_4 particles are dispersed on the GO surface and some wrinkles are observed on the surface of the composite. The zeta potentials of MGOs/SA at different pH values (2–11) are shown in Fig. S3 (Supplementary data). Zeta potential is a physical parameter commonly used to quantify the surface electrical potential of the solid particle and the stability of liquid dispersions [21]. As shown in Fig. S3, the zeta potential decreases with the increase of pH. At $pH < 4.22$, zeta potentials are positive due to the protonation reaction on the surfaces of the adsorbent. At $pH > 4.22$, the surfaces of MGOs/SA are negatively charged due to the deprotonation process [11].

3.2. Effect of initial solution pH

Solution pH is one of the most important variables affecting the adsorption process due to the pH affects the aqueous chemistry and surface binding-sites of the adsorbent [22]. Besides, the wastewaters usually have a wide range of pH values. Therefore, the pH of the aqueous solution has played a significant role in the wastewater treatment process [23]. The influences of initial solution pH on Cd(II) and aniline decontamination by MGOs/SA were studied, and the results are shown in Fig. 3. From Fig. 3A, the adsorption of Cd(II) on MGOs/SA increases with the increase of pH values from 2 to 11 in the absence of aniline. It is well known that the solution pH affects the speciation of Cd(II) and the surface charge of adsorbent. Distribution of Cd(II) species as a function of solution pH was obtained using the program visual MINTEQ and the results (Fig. 4A) demonstrate that Cd(II) presents in the form of Cd^{2+} , $Cd(OH)^+$, $Cd(OH)_2$, $Cd_2(OH)_3^+$, $Cd(OH)_3^-$ and $Cd(OH)_4^{2-}$ at various pH values. From Fig. 4A, we can see that the predominant Cd(II) species is Cd^{2+} when the $pH < 8$. From the results of the zeta potential (Fig. S3), the pH_{pzc} value for MGOs/SA is 4.22. At $pH < pH_{pzc}$, the MGOs/SA surfaces are positively charged due to the protonation reactions:



whereas at $pH > pH_{pzc}$, the MGOs/SA surfaces are negatively charged because of the deprotonation reactions:



where $\equiv C$ represents the surface of MGO/SA, $-OH$ represents hydroxyl group, and $-SO_3H$ represents the sulfo group. The uptake

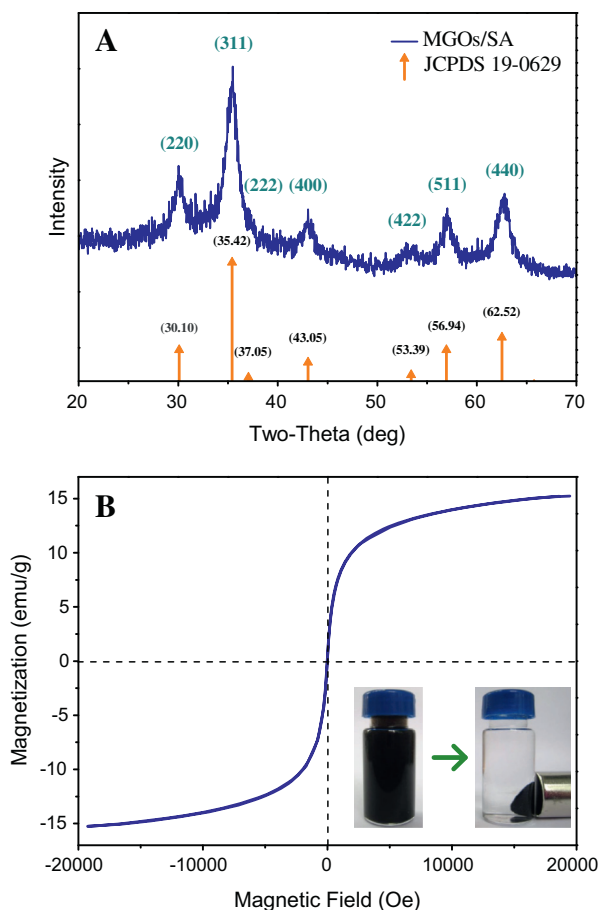


Fig. 2. Characterization of MGOs/SA: (A) XRD pattern and (B) magnetization curve at room temperature (the insets show the MGOs/SA dispersed in ultrapure water and the magnetic separation).

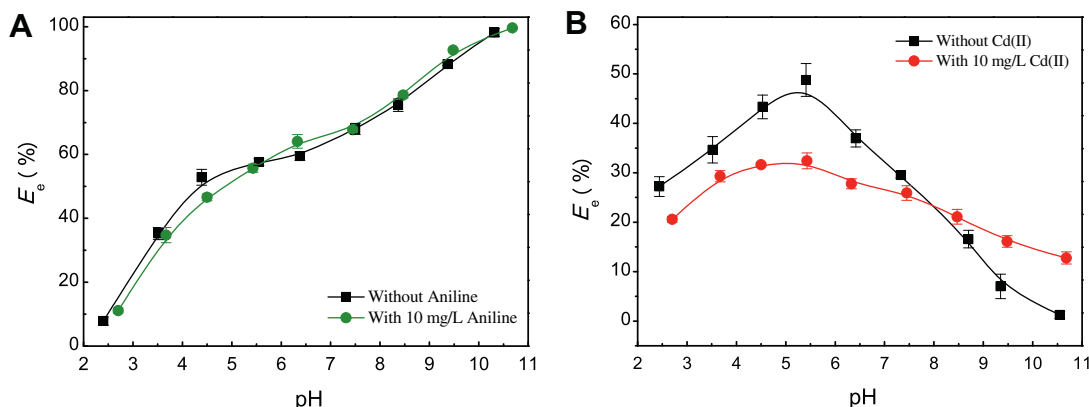


Fig. 3. Effect of the solution pH on Cd(II) (A) and aniline (B) adsorption to MGOs/SA: $m/V = 0.34$ g/L, $t = 24$ h, $C_{0(\text{Cd})} = 10$ mg/L, $C_{0(\text{aniline})} = 10$ mg/L, $T = 30$ °C.

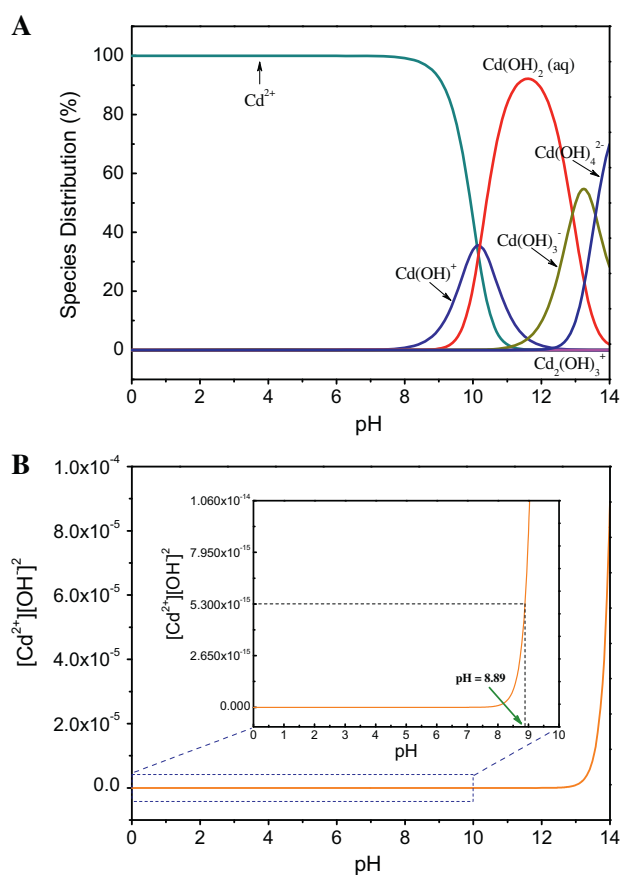
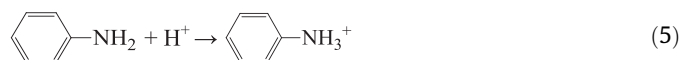


Fig. 4. (A) Distribution of Cd(II) species in solution as a function of pH computed by the program visual MINTEQ: $C_0 = 10$ mg/L, $T = 30$ °C; (B) the precipitation curve of Cd(II) at the concentration of 10 mg/L ($K_{sp} = 5.30 \times 10^{-15}$).

of Cd(II) was small at $\text{pH} < \text{pH}_{\text{pzc}}$ ($\text{pH}_{\text{pzc}} = 4.22$). The reason for this phenomenon is that the positive Cd^{2+} are difficult to adsorb on the positively charged surfaces of MGOs/SA because of the electrostatic repulsion [3]. As the pH increased, the deprotonated sites ($\equiv\text{C}-\text{O}^-$ and $\equiv\text{C}-\text{SO}_3^-$) of the MGOs/SA surfaces are more available to remove the positively charged Cd(II) ions (Cd^{2+} , $\text{Cd}(\text{NO}_3)^+$ and $\text{Cd}(\text{OH})^+$), thereby resulting in the increase of Cd(II) ions adsorption. The precipitation curve of Cd(II) calculated from the precipitation constant of $\text{Cd}(\text{OH})_2(\text{s})$ ($K_{sp} = 5.30 \times 10^{-15}$) at the concentration of 10 mg/L is shown in Fig. 4B. It is clear that Cd(II) starts to form precipitation at pH 8.89. And in the pH range of 8.89–11.0, the main

Cd(II) species are Cd^{2+} , $\text{Cd}(\text{OH})^+$, $\text{Cd}(\text{OH})_2$ and $\text{Cd}(\text{OH})_3^-$ (Fig. 4A). Therefore, at $\text{pH} > 8.89$, the high removal percentage is mainly due to the cooperating role of precipitation of $\text{Cd}(\text{OH})_2$ and adsorption of Cd^{2+} , $\text{Cd}(\text{OH})^+$, $\text{Cd}(\text{OH})_3^-$ on MGOs/SA.

The decontamination of Cd(II) ions with MGOs/SA at various pH values shows different trends in the presence of aniline (Fig. 3A). At $\text{pH} < 5.4$, the presence of aniline reduces the adsorption rate of Cd(II) ions on MGO/SA composites, due to large quantities of protonated aniline competing with Cd(II) ions for the adsorption sites. At low pH values, aniline can be protonated (Eq. (5)), and the protonated aniline can compete with Cd^{2+} for the adsorption sites ($-\text{SO}_3\text{H}$ and $-\text{OH}$), therefore reducing the adsorption capacity for Cd(II) ions.



Moreover, the amino groups ($-\text{NH}_2$) of aniline in the solution can form strong aniline-Cd(II) complexes and thereby competitively diminish the extent of Cd(II) adsorption [11]. However, the percentage of Cd(II) adsorption is enhanced in the presence of aniline at $\text{pH} > 5.4$. These phenomena can be explained by the complexation of surface-adsorbed aniline and Cd(II). Aniline can be adsorbed on the surfaces of the MGOs/SA by means of π - π electron coupling, and then the amino groups ($-\text{NH}_2$) of the adsorbed aniline can act as adsorption sites for Cd(II) ions [24]. This results in a more favorable attraction for Cd(II) ions in the solution and enhances the formation of MGO/SA-aniline-Cd ternary surface complexes [25].

The adsorption of aniline on MGOs/SA as a function of pH is shown in Fig. 3B. As can be observed from Fig. 3B, in the system without any Cd(II) ions, the aniline adsorption on MGOs/SA increases when the pH value changes from 2 to 5.5, reaches a maximum value at about pH 5.5 and then decreases with the pH increasing from 5.5 to 11. This can be explained with the protonation of the functional groups on the adsorbates as well as adsorbents [16]. Aniline is a weak base that can be protonated to form anilinium ion (Eq. (5)). Dissociated species are dominant for aniline at $\text{pH} < \text{pK}_a$ ($\text{pK}_a = 4.6$), whereas nondissociated species are dominant at $\text{pH} > \text{pK}_a$ [26]. At $\text{pH} < 4.22$, the surfaces of MGOs/SA are positively charged which can provide stronger electrostatic repulsions between anilinium ions and the adsorbents. With increasing pH, the effective concentration of the dissociated species of aniline is significantly reduced, and the positive charge content of MGOs/SA surfaces is reduced. Therefore, electrostatic repulsions between adsorbates and adsorbents are reduced, and the adsorption of aniline increases with increasing pH [26]. At $4.22 < \text{pH} < 4.6$, the MGOs/SA surfaces are negatively charged while the aniline molecules are still positively charged, then MGOs/SA and aniline can

interact via electrostatic attraction, thereby enhancing the aniline adsorption intensity [11]. The hydrogen bonding and π - π interaction are the predominant mechanisms at high pH value (pH > 4.6) where the neutral aniline molecules are the dominated species. MGOs/SA surfaces are more negatively charged at pH > 5.5 and thus can adsorb more water molecules, which can reduce the adsorption of aniline molecules. Similar finding was reported for the adsorption of aniline by PANI/MWCNTs [26].

Fig. 3B indicates that the presence of Cd(II) ions reduces aniline adsorption on MGOs/SA at pH < 7.8 but enhances the aniline adsorption at pH > 7.8. The predominant Cd(II) species is Cd²⁺ when the pH < 8 (Fig. 4A) and they can compete with aniline for the adsorption sites. This results in the reduction of aniline adsorption on MGOs/SA. It is well known that a high pH value would cause a hydrolysis process of metal cations and form metal hydroxide, such as Cd(OH)⁺ and Cd(OH)₂ [9]. The Cd(OH)₂ can act as adsorbents for the removal of aniline molecules from the solution. Therefore the presence of Cd(II) enhances aniline adsorption on MGOs/SA at high pH value.

3.3. Effect of aniline concentration

The influence of aniline concentration on Cd(II) adsorption was studied at pH = 6.00 ± 0.01. As shown in Fig. 5, the aniline concentration significantly affects Cd(II) adsorption. Cd(II) adsorption increases with increasing aniline concentration from 0 to 120 mg/L and decreases slightly with further increasing aniline concentration from 120 to 160 mg/L. Similar observation on the effects of humic substances on Pb(II) sorption to multiwalled carbon nanotubes/polyacrylamide composites has been reported [25]. The increase of Cd(II) adsorption at C_{aniline} < 120 mg/L is attributed to the complexation of Cd(II) ions with adsorbed aniline on MGOs/SA surface. The amino group on the benzene ring of aniline is known to form stable complexes with various metal ions. Aniline can be bound to MGOs/SA by means of π - π electron coupling, and more adsorption sites are available for Cd(II) adsorption. The decrease of Cd(II) removal at higher aniline concentration can be interpreted by the formation of soluble Cd(II)-aniline complexes in aqueous solution. More aniline in the aqueous solution indicates that there are fewer Cd(II)-aniline complexes on the surfaces of MGOs/SA.

3.4. Effect of ionic strength

It is well known that industrial wastewater contains not only pollutants but also high concentrations of salts, which may affect the removal of pollutants [21]. The effect of ionic strength on the

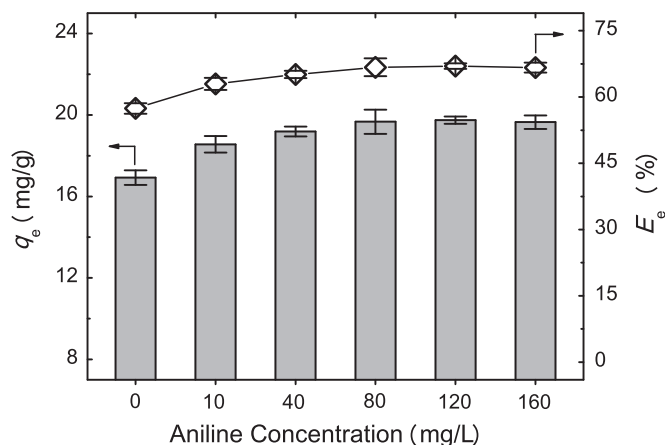


Fig. 5. Effect of aniline concentration on Cd(II) adsorption to MGOs/SA: $m/V = 0.34$ g/L, $t = 24$ h, pH = 6.00 ± 0.01, $C_{0(\text{Cd})} = 10$ mg/L, $T = 30$ °C.

decontamination of Cd(II) by MGOs/SA was studied by a series of experiments at varying concentrations of NaCl solutions in the presence of aniline. As seen from Fig. 6, the adsorption of Cd(II) on MGO/SA composites decreases as the NaCl concentration increases from 0 to 0.1 M. This can be explained in terms of four aspects. Firstly, the ionic strength of solution influenced the activity coefficient of Cd(II) ions, which limited their transfer to MGOs/SA surfaces [27]. Secondly, competition of Na⁺ ions with the Cd(II) ions for adsorption sites of MGO/SA composites resulted in the observed decrease in the uptake capacities with increasing electrolyte NaCl concentration [28]. Thirdly, the increase in NaCl concentration increased the screening effect between the positively charged Cd(II) in solution and the negative charge of the MGOs/SA surfaces, which reduced the electrostatic interactions [29]. Fourthly, the increased amount of NaCl reduced the electrostatic repulsions between MGOs/SA, leading to aggregation of MGOs/SA particles. Consequently, the amounts of available binding sites were reduced and the adsorption of Cd(II) on MGOs/SA decreased [25,30].

3.5. Adsorption kinetics

The kinetics of the adsorption describing the adsorbate uptake rate is one of the important characteristics which control the residence time of adsorbate uptake at the solid-liquid interface [31]. Hence, the kinetics of Cd(II) adsorption was carried out to investigate the adsorption behavior of the MGOs/SA. The decontamination of Cd(II) by MGOs/SA as a function of contact time in the presence of aniline is shown in Fig. 7A. It can be seen that the adsorption rate of Cd(II) is very fast during the initial 6 h, and then remain constant with further increasing contact time. Quantifying the changes in adsorption with time requires an appropriate kinetic model, and therefore pseudo-first-order, pseudo-second-order, Elovich and intraparticle diffusion were investigated and compared. Detailed information of those models is described in the Supplementary data (SD). Fig. 7A presents that the nonlinear curves of the pseudo-first-order and the pseudo-second-order models fit with the experimental data of Cd(II) adsorption. The non-linearized form of the Elovich model for the adsorption is given in Fig. S4 (SD). The kinetic parameters calculated from models are listed in Table 1. It can be seen that the pseudo-second-order model fits the experimental data better than pseudo-first-order model and Elovich model, which indicates that the chemisorption is the rate-controlling mechanism [32].

The intraparticle diffusion model was used to identify the mass transfer steps in the Cd(II) adsorption onto MGOs/SA. Fig. 7B shows q_t versus $t^{0.5}$ plot for the adsorption of Cd(II). Piecewise

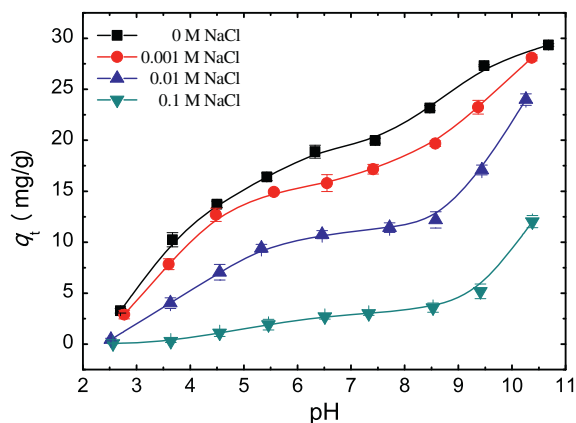


Fig. 6. Effect of ionic strength on Cd(II) adsorption onto MGOs/SA: $m/V = 0.34$ g/L, $t = 24$ h, $C_{0(\text{Cd})} = 10$ mg/L, $C_{0(\text{aniline})} = 10$ mg/L, $T = 30$ °C, $C_{0(\text{NaCl})} = 0, 0.001, 0.01,$ and 0.1 M.

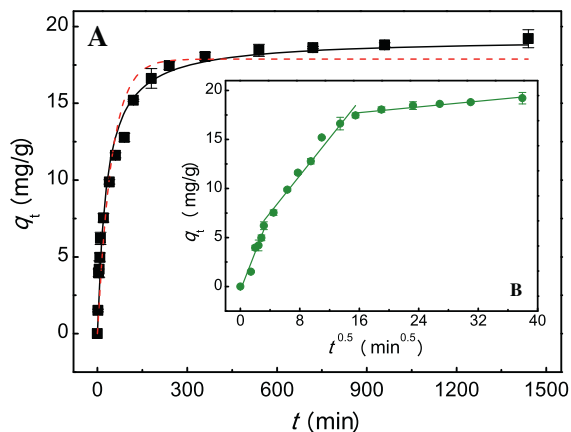


Fig. 7. (A) Time profiles of Cd(II) adsorption with MGOs/SA (the dashed line is Pseudo-first-order adsorption kinetics simulation, and the solid line is Pseudo-second-order adsorption kinetics simulation); (B) intraparticle diffusion kinetics: $m/V = 0.34$ g/L, $\text{pH} = 6.00 \pm 0.01$, $C_{0(\text{Cd})} = 10$ mg/L, $C_{0(\text{aniline})} = 10$ mg/L, $T = 30$ °C.

linear regression of the data shows that q_t versus $t^{0.5}$ plot has three distinct regions. The initial portion represents the boundary layer diffusion (film diffusion), and the second portion describes the gradual adsorption step, where the intraparticle diffusion is the rate-limiting step. The third linear portion indicates the adsorption–desorption equilibrium. Therefore, film diffusion and intraparticle diffusion simultaneously occur during the adsorption processes, and the intraparticle diffusion is not the only rate controlling step for the adsorption process [33]. Similar behavior was obtained by Zhang et al. [34] in the adsorption of Rhenium ions onto modified nano- Al_2O_3 .

3.6. Adsorption isotherms

The decontamination of Cd(II) using MGOs/SA has been studied in the absence and presence of aniline at 15, 30 and 45 °C to determine the relative parameters of adsorption isotherms. The temperature has two major effects on the adsorption process [35]. Increasing the temperature is known to increase the rate of diffusion of the adsorbate molecules across the external boundary layer and in the internal pores of the adsorbent particle, owing to the decrease in the viscosity of the solution. In addition, changing the temperature will change the equilibrium capacity of the adsorbent for a particular adsorbate [35]. As seen from Fig. 8, the adsorption capacities of MGOs/SA for Cd(II) in the absence and presence of aniline increase with the increasing temperature from 15 to 30 °C and decrease with further increase of the temperature to 45 °C. From the results of the kinetic studies, we can get that both chemisorption and physisorption are involved in the adsorption process. At low temperatures, chemisorption is negligible, and the physisorption plays a predominant role in the adsorption of Cd(II), resulting in the low adsorption capacities for Cd(II). Higher temperatures can accelerate the rate of diffusion of the Cd(II) ions from the bulk liquid to the surfaces of the MGOs/SA, and enhance the chemical interaction between the Cd(II) ions and the MGOs/SA

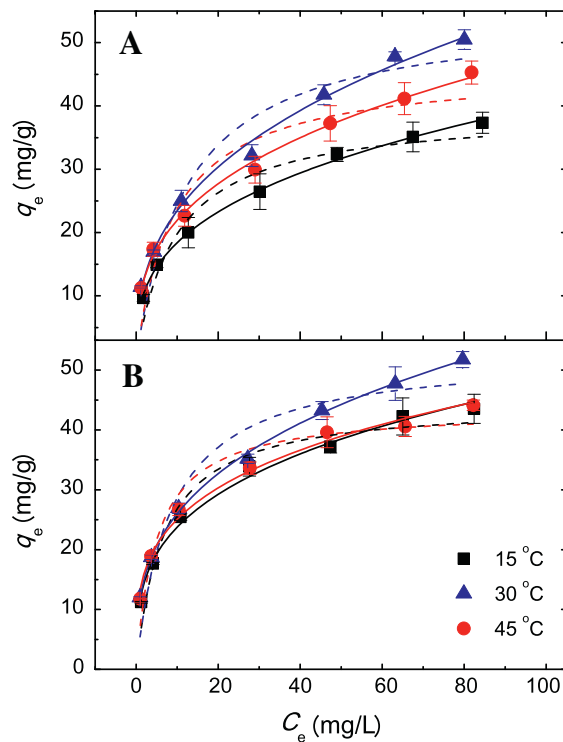


Fig. 8. Langmuir (dashed line) and Freundlich (solid line) adsorption isotherms for Cd(II) adsorption onto MGOs/SA in the absence (A) and presence (B) of aniline at three different temperatures: $m/V = 0.34$ g/L, $t = 24$ h, $\text{pH} = 6.00 \pm 0.01$, $C_{0(\text{aniline})} = 10$ mg/L (only for B), $T = 15, 30$, and 45 °C.

surfaces, which may partly contribute to the increase of adsorption capacities at higher temperatures. However, further raising the temperature to 45 °C leads to the decrease of adsorption capacities likely because the physical interactions between Cd(II) ions and the surfaces of MGOs/SA are reduced.

To better understand of the adsorption mechanisms, the Langmuir, Freundlich and Temkin models, which are described in the Supplementary data (SD), were applied to simulate the experimental data. The Langmuir and Freundlich adsorption isotherms obtained using the nonlinear method at 15, 30, and 45 °C are shown in Fig. 8, and the relative parameters calculated from the two models are listed in Table 2. From Fig. 8 and Table 2, we can see that the experimental data are fitted better by the Freundlich model than by the Langmuir model within the studied temperature range. Özcan et al. [36] also reported that Freundlich adsorption model better explained the adsorption of AR57 and AB294 onto acid-activated bentonite. The Freundlich constant K_F indicates the adsorption capacity of the adsorbent. From Table 2, the K_F values for Cd(II) adsorption onto MGOs/SA without aniline are 8.46 ± 0.30 , 9.97 ± 0.68 and 10.12 ± 0.50 at 15, 30, and 45 °C, respectively. In the system with aniline, the values of K_F are 11.92 ± 0.75 , 12.16 ± 0.30 and 13.37 ± 0.79 at 15, 30, and 45 °C, respectively. All the values of K_F in the system with aniline are higher than the K_F values in the system without aniline, indicating that the aniline in the system can enhance the adsorption capacity

Table 1
Parameters obtained from different kinetic models.

Pseudo-first-order		Pseudo-second-order		Elovich	
$k_1 \times 10^2$ (1/min)	2.13 ± 0.30	$k_2 \times 10^3$ (g/mg min)	1.73 ± 0.21	α (mg/g min)	2.47 ± 0.37
q_e (mg/g)	17.87 ± 0.59	q_e (mg/g)	19.20 ± 0.42	β (g/mg)	0.335 ± 0.014
R^2	0.945	h (mg/g min)	0.638	R^2	0.978
		R^2	0.982		

Table 2
Isotherm constants for adsorption of Cd(II) onto MGOs/SA in the absence and presence of aniline.

	Absence of aniline			Presence of aniline		
	15 °C	30 °C	45 °C	15 °C	30 °C	45 °C
<i>Langmuir isotherm</i>						
q_{\max} (mg/g)	39.24 ± 2.62	54.83 ± 5.34	45.92 ± 4.27	44.57 ± 2.32	52.79 ± 4.20	43.50 ± 2.25
K_L (L/mg)	0.102 ± 0.027	0.081 ± 0.029	0.107 ± 0.041	0.151 ± 0.036	0.119 ± 0.040	0.199 ± 0.051
R^2	0.935	0.910	0.881	0.948	0.912	0.935
<i>Freundlich isotherm</i>						
K_F	8.46 ± 0.30	9.97 ± 0.68	10.12 ± 0.50	11.92 ± 0.75	12.16 ± 0.30	13.37 ± 0.79
n	2.96 ± 0.08	2.69 ± 0.13	2.97 ± 0.12	3.34 ± 0.18	3.03 ± 0.06	3.66 ± 0.21
R^2	0.997	0.992	0.995	0.989	0.999	0.988
<i>Temkin isotherm</i>						
a_T (L/g)	1.68 ± 0.42	1.81 ± 0.76	2.34 ± 0.97	2.74 ± 0.53	2.66 ± 0.95	4.07 ± 0.77
b_T (kJ/mol)	0.331 ± 0.023	0.267 ± 0.030	0.334 ± 0.035	0.304 ± 0.015	0.297 ± 0.025	0.359 ± 0.015
R^2	0.973	0.929	0.939	0.987	0.955	0.989

for Cd(II) at pH 6.00. The magnitude of Freundlich constant n is also an indication of the favorability of adsorption [37]. Previous research pointed out that n values between 1 and 10 represent beneficial adsorption based on mathematical calculations [38]. All the values of Freundlich constant n (Table 2) in this study are within the beneficial adsorption range, which indicates that MGOs/SA can be used as effective adsorbents.

The Temkin isotherm plots are demonstrated in Fig. S5 (SD), and the Temkin constants are given in Table 2. Temkin isotherm generates a satisfactory fit to the experimental data as indicated by correlation coefficients. Typical bonding energy range for ion-exchange mechanism is reported to be in the range of 8–16 kJ/mol while physisorption processes are reported to have adsorption energies less than -40 kJ/mol [39]. The values of b_T for Cd(II) adsorption onto MGOs/SA in the absence of aniline are 0.331 ± 0.023 , 0.267 ± 0.030 and 0.334 ± 0.035 at 15, 30, and 45 °C, respectively. In the system with aniline, the b_T values are 0.304 ± 0.015 , 0.297 ± 0.025 and 0.359 ± 0.015 at 15, 30, and 45 °C, respectively. All of these values are out of the two ranges, which indicates that the adsorption processes seem to involve chemisorption and physisorption. The results are similar to the adsorption of Cr(VI) on ethylenediamine-modified cross-linked magnetic chitosan resin [40].

4. Conclusions

The MGOs/SA exhibit superparamagnetic behavior and can be easily separated by magnetic separation from the medium after adsorption. The presence of aniline can affect the adsorption of Cd(II) on MGOs/SA, and conversely Cd(II) can also influence the aniline adsorption. Cd(II) and aniline adsorption are influenced by the pH of aqueous solution due to that the pH affects the surface charge of the MGOs/SA and the speciation of Cd(II) and aniline. Besides, the increasing ionic strength has a negative impact on the adsorption capacities of MGOs/SA. The results of adsorption kinetics study illustrated that Cd(II) adsorption follows the pseudo-second-order model and the chemisorption is the rate-controlling mechanism. Both film diffusion and intraparticle diffusion simultaneously occur during the adsorption process. Besides, the isotherm experiment data can be well described with Freundlich, and both chemisorption and physisorption are involved in the adsorption process. This research indicates that MGO/SA composites are very suitable materials for metal ions and organic matters pollution cleanup.

Acknowledgments

The authors would like to thank financial support from the National Natural Science Foundation of China (41271332), the

Hunan Provincial Innovation Foundation For Postgraduate (CX2012B138), the Natural Science Foundation of Hunan province, China (11JJ2031) and the Science and Technology Planning Project of Hunan Province, China (2012SK2021).

Appendix A. Supplementary material

Supplementary data associated with this article can be found, in the online version, at <http://dx.doi.org/10.1016/j.jcis.2014.04.016>.

References

- [1] C.L. Chen, X.K. Wang, *Ind. Eng. Chem. Res.* 45 (2006) 9144.
- [2] U. Garg, M.P. Kaur, G.K. Jawa, D. Sud, V.K. Garg, *J. Hazard. Mater.* 154 (2008) 1149.
- [3] G.X. Zhao, J.X. Li, X.M. Ren, C.L. Chen, X.K. Wang, *Environ. Sci. Technol.* 45 (2011) 10454.
- [4] S. Bai, X.P. Shen, X. Zhong, Y. Liu, G.X. Zhu, X. Xu, K.M. Chen, *Carbon* 50 (2012) 2337.
- [5] Z. Yang, S.S. Ji, W. Gao, C. Zhang, L. Ren, W.W. Tjiu, Z. Zhang, J.S. Pan, T.X. Liu, *J. Colloid Interface Sci.* 408 (2013) 25.
- [6] Y. Zhang, Y. Cheng, N. Chen, Y. Zhou, B. Li, W. Gu, X. Shi, Y. Xian, *J. Colloid Interface Sci.* 421 (2014) 85.
- [7] L.-Z. Bai, D.-L. Zhao, Y. Xu, J.-M. Zhang, Y.-L. Gao, L.-Y. Zhao, J.-T. Tang, *Mater. Lett.* 68 (2012) 399.
- [8] M.C. Liu, C.L. Chen, J. Hu, X.L. Wu, X.K. Wang, *J. Phys. Chem. C* 115 (2011) 25234.
- [9] C.J. Madarang, H.Y. Kim, G.H. Gao, N. Wang, J. Zhu, H. Feng, M. Gorring, M.L. Kasner, S.F. Hou, *ACS Appl. Mater. Interfaces* 4 (2012) 1186.
- [10] H.L. Ma, Y.W. Zhang, Q.H. Hu, D. Yan, Z.Z. Yu, M.L. Zhai, *J. Mater. Chem.* 22 (2012) 5914.
- [11] J. Li, S.W. Zhang, C.L. Chen, G.X. Zhao, X. Yang, J.X. Li, X.K. Wang, *ACS Appl. Mater. Interfaces* 4 (2012) 4991.
- [12] X.Y. Lin, J.P. Zhang, X.G. Luo, C. Zhang, Y. Zhou, *Chem. Eng. J.* 172 (2011) 856.
- [13] H.Q. Tang, J. Li, Y.Q. Bie, L.H. Zhu, J. Zou, *J. Hazard. Mater.* 175 (2010) 977.
- [14] S.T. Yang, Y.L. Chang, H.F. Wang, G.B. Liu, S. Chen, Y.W. Wang, Y.F. Liu, A.N. Cao, *J. Colloid Interface Sci.* 351 (2010) 122.
- [15] G.F. Chen, S.Y. Zhai, Y.L. Zhai, K. Zhang, Q.L. Yue, L. Wang, J.S. Zhao, H.S. Wang, J.F. Liu, J.B. Jia, *Biosens. Bioelectron.* 26 (2011) 3136.
- [16] L. Guo, G.Y. Li, J.S. Liu, P. Yin, Q. Li, *Ind. Eng. Chem. Res.* 48 (2009) 10657.
- [17] S.T. Yang, J.X. Li, Y. Lu, Y.X. Chen, X.K. Wang, *Appl. Radiat. Isot.* 67 (2009) 1600.
- [18] X. Lv, X. Xue, G. Jiang, D. Wu, T. Sheng, H. Zhou, X. Xu, *J. Colloid Interface Sci.* 417 (2014) 51.
- [19] C.Y. Hou, Q.H. Zhang, M.F. Zhu, Y.G. Li, H.Z. Wang, *Carbon* 49 (2011) 47.
- [20] L.Z. Bai, D.L. Zhao, Y. Xu, J.M. Zhang, Y.L. Gao, L.Y. Zhao, J.T. Tang, *Mater. Lett.* 68 (2012) 399.
- [21] J. Xu, L. Wang, Y.F. Zhu, *Langmuir* 28 (2012) 8418.
- [22] B.H. Hameed, M.I. El-Khaiary, *J. Hazard. Mater.* 159 (2008) 574.
- [23] A. Khaled, A. El Nembr, A. El-Sikaily, A. Abdelwahab, *Desalination* 238 (2009) 210.
- [24] T. Wu, X. Cai, S. Tan, H. Li, J. Liu, W. Yang, *Chem. Eng. J.* 173 (2011) 144.
- [25] S.B. Yang, J. Hu, C.L. Chen, D.D. Shao, X.K. Wang, *Environ. Sci. Technol.* 45 (2011) 3621.
- [26] D.D. Shao, J. Hu, C.L. Chen, G.D. Sheng, X.M. Ren, X.K. Wang, *J. Phys. Chem. C* 114 (2010) 21524.
- [27] C. Ravat, J. Dumonceau, F. Monteil-Rivera, *Water Res.* 34 (2000) 1327.
- [28] X.S. Wang, J. Huang, H.Q. Hu, J. Wang, Y. Qin, *J. Hazard. Mater.* 142 (2007) 468.
- [29] C. Moreno-Castilla, M.A. Alvarez-Merino, M.V. Lopez-Ramon, J. Rivera-Utrilla, *Langmuir* 20 (2004) 8142.
- [30] K.L. Mercer, J.E. Tobiason, *Environ. Sci. Technol.* 42 (2008) 3797.

- [31] J.H. Zhu, S.Y. Wei, H.B. Gu, S.B. Rapole, Q. Wang, Z.P. Luo, N. Haldolaarachchige, D.P. Young, Z.H. Guo, *Environ. Sci. Technol.* 46 (2012) 977.
- [32] Y.S. Ho, Adsorption of Heavy Metals from Waste Streams by Peat, Ph.D. Thesis, University of Birmingham, Birmingham, UK, 1995.
- [33] X.J. Hu, Y.G. Liu, H. Wang, A.W. Chen, G.M. Zeng, S.M. Liu, Y.M. Guo, X. Hu, T.T. Li, Y.Q. Wang, L. Zhou, S.H. Liu, *Sep. Purif. Technol.* 108 (2013) 189.
- [34] L. Zhang, X.Q. Jiang, T.C. Xu, L.J. Yang, Y.Y. Zhang, H.J. Jin, *Ind. Eng. Chem. Res.* 51 (2012) 5577.
- [35] Z. Al-Qodah, *Water Res.* 34 (2000) 4295.
- [36] A.S. Özcan, A. Özcan, *J. Colloid Interface Sci.* 276 (2004) 39.
- [37] Y.R. Wang, W. Chu, *Ind. Eng. Chem. Res.* 50 (2011) 8734.
- [38] R.E. Treybal, *Mass Transfer Operations*, McGraw-Hill Higher Education, New York, 1980.
- [39] B. Kiran, A. Kaushik, *Biochem. Eng. J.* 38 (2008) 47.
- [40] X.J. Hu, J.S. Wang, Y.G. Liu, X. Li, G.M. Zeng, Z.L. Bao, X.X. Zeng, A.W. Chen, F. Long, *J. Hazard. Mater.* 185 (2011) 306.